

Mode II fracture energy and interface law for FRP – concrete bonding with different concrete surface preparations

M. Savoia, C. Mazzotti & B. Ferracuti

DISTART – Structural Engineering, University of Bologna, Bologna, Italy

ABSTRACT: Results of an experimental campaign on delamination of CFRP sheets and plates bonded to concrete are presented. In particular, the effect of different surface preparations (grinding or, alternatively, sand blasting) is investigated. Six specimens have been tested by using a particular experimental set-up where the CFRP reinforcement is bonded to concrete and its back side is fixed to an external restraining system. The adopted set-up allows for a stable delamination process, with progressive transition between two limit states (perfect bonding and fully delaminated plate). Both strain gages along the FRP plate and LVDT transducers have been used. Experimental results showed that the technique for surface preparation may have a significant influence on the value of mode II fracture energy. Starting from experimental data, non linear interface laws have been calibrated. It is shown that, when concrete surface has been prepared by sand blasting, high values of fracture energy are attained with a smaller value of peak shear stress and significantly higher slips. Moreover, FRP – concrete interface law exhibits a less brittle behavior of the softening branch.

1 INTRODUCTION

When using FRP (Fibre Reinforced Plastic) plates or sheets to strengthen r.c. beams, bonding is very important. Since delamination is a very brittle failure mechanism, it must be avoided in practical applications. Bonding depends on mechanical and physical properties of concrete, composite and adhesive.

Moreover, it is well known that concrete surface preparation and bonding technique are very important for a correct application, in order to avoid premature failures. In recent Italian CNR DT 200/2004 Guidelines (2006) for design of strengthening interventions with FRP, when FRP application is done using certified methods, smaller design coefficients reducing bond strength are allowed. Nevertheless, very few studies can be found on the effect of different preparations of concrete surface before bonding (Toutanji & Ortiz 2001). In Matana et al. (2005), bond strength in peel-off tests has been measured; using different surface treatments, laser profilometer has been used to measure concrete surface roughness (Galecki et al. 2001).

Recent design Guidelines consider mode II fracture energy as the most important material parameter when estimating delamination failure load. Following analogous proposals for mode II fracture energy of concrete, fracture energy of FRP-concrete interface is written as a function of concrete strength through a parameter which must be calibrated ex-

perimentally (Ferracuti et al. 2007a). Nevertheless, since that expression has been calibrated considering all delamination data together, with concrete strength as the only material parameter, coefficient of variation of results is very high and, consequently, design value of fracture energy is much lower than mean value. In order to reduce data scattering, more information of dependence of fracture energy on material parameters are necessary.

In the present paper, a set of experimental results on delamination of FRP reinforcements bonded to concrete is presented. Both CFRP plates and sheets have been tested. Moreover, three different treatments of concrete surface before bonding have been considered: grinding with two types of stone wheel giving different surface roughness or, alternatively, sand blasting.

Tests have been performed by adopting a new experimental set-up, recently developed by the authors, allowing for a stable delamination process. Specimen back-side is fixed to an external retaining system, i.e. concrete and CFRP reinforcement in that section have null displacement. Then, a very stable delamination process occurs at constant applied force, corresponding to delamination force of an anchorage of infinite length. That value is then used to define mode II fracture energy of interface law.

Moreover, a number of closely spaced strain gages is placed along the FRP plate to measure strains. Then, starting from experimental data, aver-

age shear stresses between two subsequent strain gages and corresponding shear slips have been computed. These data have been used to calibrate non linear interface laws, according to the procedure described in Savoia et al. (2003) and Ferracuti et al. (2007b).

It is shown that sand blasting of concrete surface gives higher values of mode II fracture energy and correspondingly, of delamination load. Nevertheless, peak shear stress is lower, and higher compliance of FRP-concrete interface is observed. Moreover, softening branch after the attainment of peak shear stress is less brittle. When grinding with stone wheel is used to remove mortar from concrete surface, roughness of the surface and, correspondingly, shear fracture energy are larger than with sand blasting.

Finally, specific fracture energy for sheets bonded to concrete is significantly higher than obtained in the case of CFRP plates.

2 MODE II SHEAR FRACTURE FOR FRP – CONCRETE BONDING

According to theoretical fracture mechanics, fracture propagation direction is governed by the criterion of the maximum release rate (van Mier 1997), as a consequence of basic laws of thermodynamics. Then, usually cracks in concrete specimens are related to tensile failure (Mode I fracture energy being the minimum), and crack propagation direction from the notch tip is taken as normal to the maximum principal stress (van Mier 1997). Also in shear-loaded beams with a start notch in the Mode II direction (Arrea & Ingraffea 1982), if a wide zone of beam is subject to shear, crack typically deviates from Mode II fracture direction to that of maximum principal stress.

Nevertheless, Mode II or shear fracture failures may occur when a narrow region is subject to high shear stresses. For instance, in Bazant & Pfeiffer (1986), shear fracture has been observed in shear-loaded beams with starting notches similar to those tested by Arrea & Ingraffea (1982), but with much smaller distance between applied shear forces: in this case, according to the criterion of the maximum release rate, cracks cannot deviate into a low stress zone of the material, because they would release little energy.

As clearly described in Bazant & Pfeiffer (1986), shear fracture initially forms as a zone of inclined tensile microcracks. Full shearing failure then requires inclined struts between microcracks be finally crushed in compression.

The failure mechanism at the micro-level explain why Mode II fracture energy G_f^{II} is far larger than Mode I (G_f^{I}), even 25 times according to Bazant & Pfeiffer (1986). For concrete specimens, G_f^{I} can be considered as a basic material constant whereas G_f^{II}

is not, since it can be calculated on the basis of G_f^{I} , tensile and concrete strength and crack band width.

When a plate is bonded to a concrete specimen and is subject to axial load up to failure, Mode II shear failure occurs (Buyukozturk et al. 2004). In fact, only a small layer of concrete close to the interface is subject to very high shear stresses (see Fig. 1), and criterion of the maximum release rate requires that fracture propagates along it. During delamination, the portion of concrete where shear stresses are transmitted is in fact very small, about 20 centimetres long and 3-5 centimetres depth.

Failure mechanism is similar as described before: according to Mohr-Coulomb criterion, inclined microcracks start locally in mode I condition in the small external layer of concrete because tensile strength is much lower than in adhesive (see Fig. 2). Inclined cracks cannot propagate more than few millimetres inside the concrete specimen, because stresses decrease very rapidly with depth from FRP-concrete interface. Then, a series of inclined struts clamped to concrete substrate are subject to com-

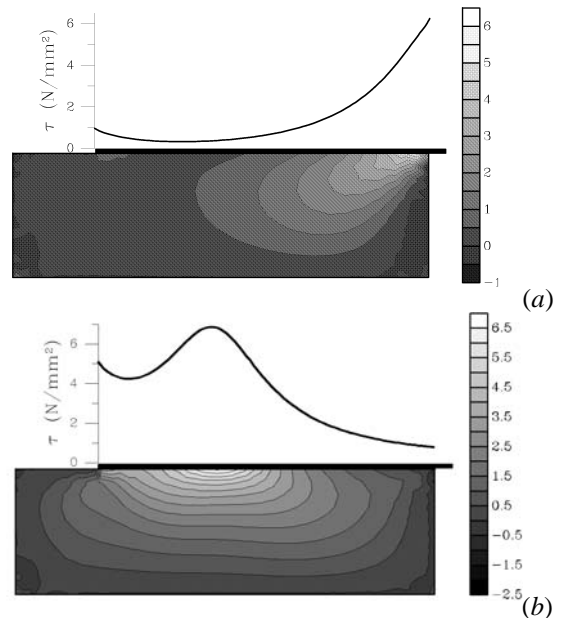


Figure 1. Shear stresses in concrete specimen for FRP plate subject to axial loading calculated at (a) 40 percent and (b) 100 percent of delamination load (from Freddi et al. 2004).

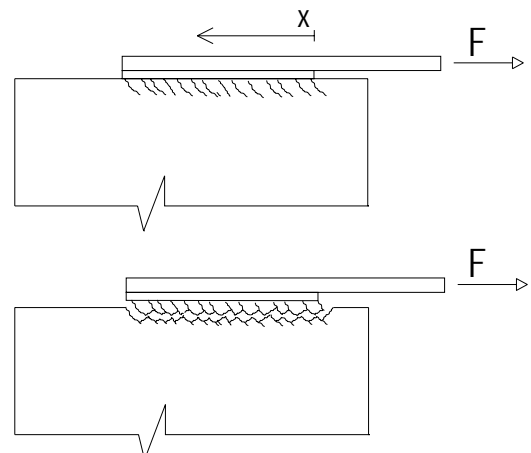


Figure 2. Mode II failure mechanism at the interface level between concrete and FRP reinforcement.

pression and bending. Final failure can be due concrete crushing in compression or transverse cracking on tensile side of concrete struts, depending on dimensions of struts, and a corrugated debonding surface parallel to the interface is typically detected after failure.

As confirmed by several experimental studies (Lu et al. 2005, Ferracuti et al. 2007a), fracture energy due to FRP – concrete debonding is much higher than Mode I fracture energy of concrete. Moreover, Mode II fracture energy may be higher than for plain concrete, due to penetration of adhesive in the concrete external layer.

Characteristics of debonding failure mechanism explain why mechanical properties of the adhesive, adhesive – concrete compatibility and concrete surface preparation before adhesive application may be very important to increase maximum load against debonding.

Statistical studies on fracture energy of FRP-concrete interface revealed very high coefficient of variation between results obtained from different specimens having same concrete tensile and compression strengths (Ferracuti et al. 2007a), whereas variation is much lower if the same surface preparation and adhesive are adopted.

3 THE EXPERIMENTAL TESTS

3.1 Mechanical properties of concrete and FRP composites

Plate – concrete bonding with different surface preparation has been investigated. CFRP sheets and plates have been bonded to concrete blocks and subject to increasing values of axial force up to complete delamination.

Concrete block dimensions were 150×200×600 mm. They were fabricated using normal strength concrete. Concrete was poured into wooden forms and externally vibrated. The top was steel-troweled.

Mean compressive strength $f_{cm} = 52.7$ MPa from compression tests and mean tensile strength $f_{ctm} = 3.81$ MPa from Brasilian tests have been obtained on cylinders at an age of 20 months. Mean value of elastic modulus was $E_{cm}=30700$ MPa.

For composites plates, CFRP sheets and plates have been used (Fig. 3a); in Table 1, type and properties of reinforcement have been reported.

A total of ten delamination tests has been per-

Table 1. Type and properties of FRP reinforcements considered in experimental tests.

Specimen	Type of Reinforcement	Width b_p (mm)	Thickness h_p (mm)	E_p (MPa)	Surface prep.
P5	Sheet Sika	80	0.13	284000	s. b.
P8	Wrap Hex 230C	80	0.13	291000	gr. 1
P9	Plate Sika	80	1.2	197000	s. b.
P1	Carbodur S	80	1.2	165000	gr. 1
P6		80	1.2	195000	gr. 2

formed, two for each type of different reinforcement and surface preparation.

In the present experimental investigation, the plate bonded length starts 100 mm from the front side of specimen and total bonded length is 500 mm (i.e. plate covers the whole concrete block length (Fig. 3b). Previous experimental investigations (Mazzotti et al. 2004) showed that this particular test setup provides for a bond stress-slip behaviour less affected by boundary conditions and more representative of the material behaviour far from cracked sections (i.e. as in the case of plate end debonding).

3.2 Surface preparation

Three different techniques for surface preparation have been adopted in order to study the effect of the treatment on delamination force and fracture energy of interface law:

Sand Blasting: Concrete surfaces have been sand blasted in order to remove the whole mortar over the aggregates, so obtaining a very rough (and slightly damaged) concrete surface.

Grinding 1: Top surfaces of concrete blocks have been grinded with a stone wheel to remove the top

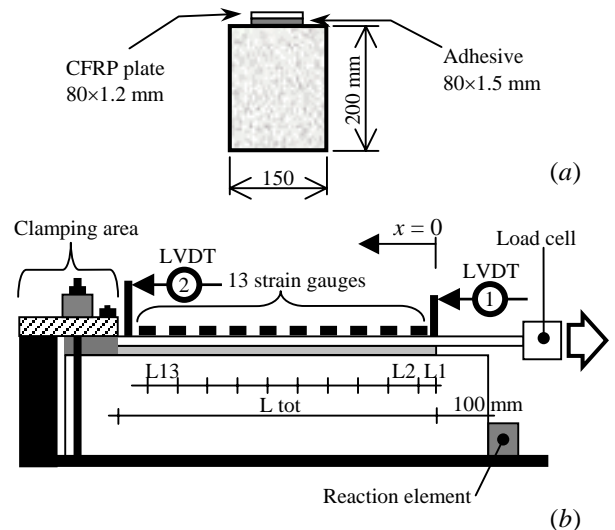


Figure 3. Experimental set-up: (a) Specimen transverse section and (b) side view with instrument positions and CFRP plate clamping system.

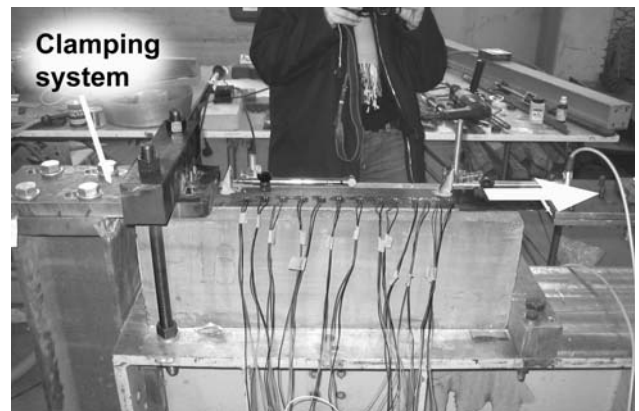


Figure 4. Experimental set-up: view of the clamping system for concrete and CFRP at the opposite sides of the specimen.

layer of mortar, just until the aggregate was visible (approximately 1 mm); due to very small dimensions of marble powder glued to the wheel, finished surface was very smooth.

Grinding 2: Top surfaces have been grinded by using a different stone wheel, characterized by a coarse iron powder able to provides for a rough finished surface.

3.3 The experimental setup

With classical set-ups (Yao et al. 2005, Ferracuti et al. 2006), complete delamination occurs during a snap-back branch. It is not possible to conduct stable measures because delamination is then a dynamic event, due to instantaneous release of elastic energy of the plate when applied load decreases.

A recently developed experimental setup (Mazzotti et al. 2004) for delamination tests has been adopted. Previous studies showed that this setup allows for a stable and controlled delamination, very important to correctly estimate delamination force as well as to measure strains in FRP during delamination.

The concrete block is positioned on a rigid frame with a front side steel reaction element 60 mm high, to avoid global horizontal translation. Moreover a steel apparatus is clamped to the back side of the specimen in order to prevent, in that section, displacements of both concrete and FRP (Fig. 4).

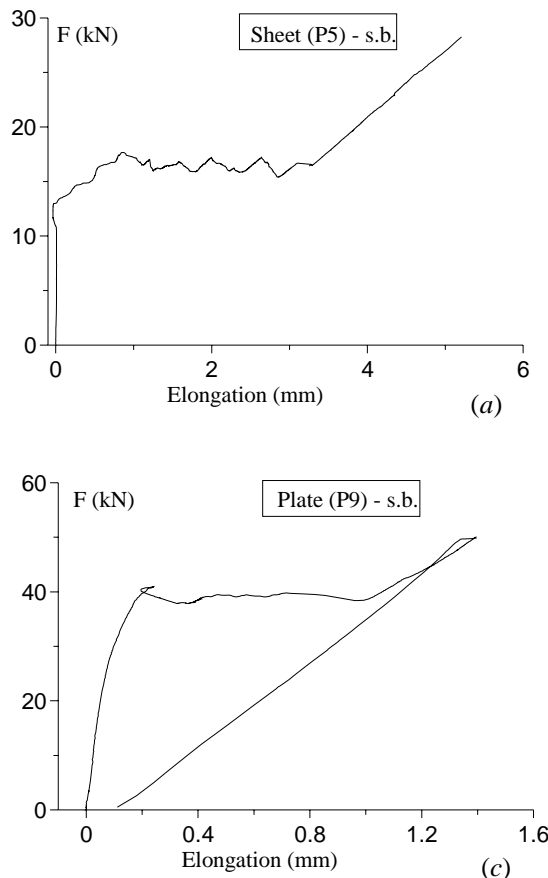


Table 2. Spacing between strain gauges (mm) along the CFRP plate.

L1	L2	L3	L4	L5	L6	L7	L8	L9	L10	L11	L12	L13
10	20	20	20	30	30	30	30	30	30	30	30	30

Table 3. Levels of applied force (kN) corresponding to FRP – strain profiles in Figure 3.

Specimen	F1	F2	F3	F4	F5	F6	F7	F8	F9	F10	F11	F12
Sheet (P5A)	2	4	6	8	10	12	14	16	18	20		
Plate (P9A)	4	8	12	16	20	24	28	32	38	42	44	46

Bonded length L_{tot} from initial to clamped section is 350 mm. In order to apply the load, the opposite side of the reinforcement is mechanically clamped with a two steel plates system free to rotate around the vertical axis. Traction force is then applied to the steel plate system by using a mechanical actuator (Fig. 3b). Tests are then performed under displacement control of the plate free end.

3.4 Instrumentation

A load cell is used to measure the applied traction force during the test. Along the CFRP, a series of thirteen strain gauges is placed on the centerline. In Table 2, spacing between strain gauges is reported, starting from the traction side of bonded part of CFRP plate/sheet. Two LVDTs are also placed at the opposite sides of bonded length in order to measure CFRP elongation and to verify the effectiveness of the clamping system (Fig. 3b).

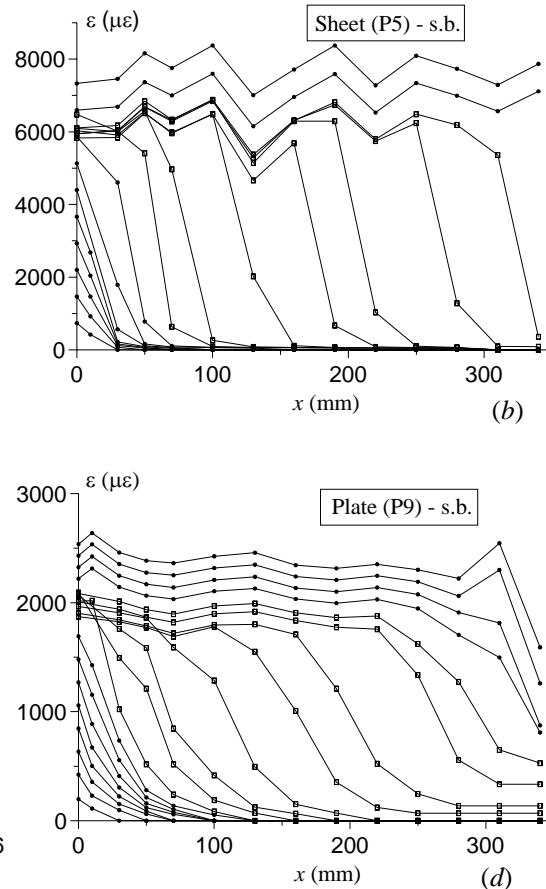


Figure 5. Results from delamination tests on FRP sheets and plates bonded to concrete: (a,c) force – plate elongation curves, (b,d) strains along FRP reinforcement at different levels of applied force, before and during delamination (s.b. = sand blasting).

4 RESULTS OF DELAMINATION TESTS

4.1 The experimental results

Tests have been carried out by performing a first load cycle up to 10 kN of traction force, followed by a monotonic loading at a rate of about 0.2 kN/s. During delamination, plate free end displacement rate was about 50 $\mu\text{m}/\text{s}$, with tests conducted under displacement control.

In Figure 5 results obtained for two specimens with CFRP sheet and plate, respectively, bonded to concrete surface previously subject to sand blasting treatment are reported (specimens P5A, P9A, respectively). In Figures 5a, c force – CFRP elongation curves of two specimens are reported. Plate elongation is measured as the difference between displacements of initial and end sections of the bonded plate (see Fig. 3). In both cases, three main behaviors can be identified: the first branch is almost linear up to 70-80 percent of maximum transmissible force. Beyond that value, stiffness degradation occurs up to the onset of delamination, when shear strength is attained at the beginning of bonding length. Subsequent delamination occurs at an almost constant value of applied force. Duration of delamination process during test was about 15 seconds. Finally, at the end of complete delamination, the only load-carrying element is the CFRP reinforcement, properly fixed at the extremity, whose behavior is linear elastic.

Some analogies with the tension-stiffening effect can be drawn. Prior to delamination, the specimen is in an uncracked state (usually defined as *State I*, where both concrete and reinforcement contribute to specimen stiffness). After complete delamination, only CFRP carries the applied load (*State II*); delamination process links these two limit states.

Effectiveness of the clamping system was verified by measurement of absolute displacement of the plate close to restrained section. Maximum displacement recorded by LVDT2 during test was about 0.15 mm.

Longitudinal strain profiles along the CFRP at different loading levels are reported in Figures 5b, d, for sheet and plate bonded to concrete, respectively. Strains at $x=0$ are obtained from values of external applied force as $\varepsilon_0 = F / E_p A_p$.

Before delamination, FRP strain profile is given by an exponential decay from the loaded extremity up to the end of effective bonding length, where strains are almost zero. When a portion of CFRP is delaminated, no shear stresses are transmitted at the interface level and axial strains are almost constant. In all tests, stable delamination process from the loaded to the clamped end has been clearly observed. Finally, when the whole reinforcement is delaminated, FRP strains are constant along the plate

and they grow up linearly together with the applied load.

4.2 Fracture energy of interface law

A further advantage of the proposed set-up is the possibility of obtaining a very stable value of maximum force at delamination F_{\max} , corresponding to the asymptotic value of transmissible force by an anchorage of infinite length. Values of delamination forces for ten tests are reported in Table 4. Making use of the following relation (see for instance Brosen 2001, Savoia et al. 2003):

$$F_{\max} = b_p \sqrt{2 E_p h_p G_f}, \quad (1)$$

where E_p , h_p , b_p are elastic modulus, thickness and width of the reinforcement, respectively, mode II fracture energy G_f of interface law can be obtained from the value of maximum transmissible force F_{\max} (see Table 3). Equation (1) is valid for every non linear interface law.

It is worth noting that, if sand blasting is used to remove the top layer of mortar on concrete surface, delamination force is about 15-20 percent greater than grinding the surface with a stone wheel with marble sand (type 1 grinding). In fact, in the first case epoxy resin may penetrate much better in external layer of concrete, even if concrete surface is slightly damaged. On the contrary, with type 1



(a)



(b)

Figure 6. Fracture surfaces at the interface level of FRP – concrete specimens after debonding, with different surface preparations before adhesive application: (a) sand blasting and (b) grinding with a stone wheel with marble sand (type 1 grinding).

Table 4. Delamination forces and fracture energy for different concrete surface preparations.

Specimen	Type	F_{\max} (kN)	F_{mean} (kN)	G_f (MPa mm)
P5A	Sheet-sand blasted	16.50	16.95	0.6087
P5B	Sheet-sand blasted	17.40		
P8A	Sheet-grinded 1	14.40	14.50	0.4341
P8B	Sheet-grinded 1	14.60		
P9A	Plate-sand blasted	37.60	38.35	0.4901
P9B	Plate-sand blasted	39.10		
P1A	Plate-grinded 1	34.50	34.00	0.3903
P1B	Plate-grinded 1	33.50		
P6A	Plate-grinded 2	41.00	39.50	0.5204
P6B	Plate-grinded 2	38.00		

grinding, concrete surface before adhesive application is very smooth, and interface discontinuity is more pronounced.

This is confirmed by comparison of fracture surfaces after delamination obtained with surface preparation by sand blasting or alternatively stone grinding (see Fig. 6). In the first case (sand blasting), the characteristic inclined cracks on the concrete surface are evident, and a significantly thick and rough layer of concrete is attached to the plate after debonding. In the second case, a thinner layer of concrete is attached to the adhesive, and in some portions there is no concrete at all. Of course, the more irregular the concrete surface after debonding, the higher the mode II fracture energy, as confirmed

by results reported in Table 4.

Finally, if grinding is realized with iron powder (type 2), giving a very rough surface with mortar completely removed from aggregate surface, fracture energy is even slightly greater than with sand blasting.

Results reported in Table 4 also show that fracture energy obtained in delamination tests on FRP sheets is 10-25 percent higher than for plates. This is probably due to vanishing in-plane stiffness of FRP sheets with respect to pultruded plates, allowing for a higher redistribution of stresses at the interface level.

5 POST-PROCESSING OF EXPERIMENTAL DATA

Strain data along the FRP plate at different loading levels are used to calculate shear stress – slip data. The origin of the x -axis is taken at the origin of the bonded plate. Considering an elastic behavior for the composite, the average value of shear stress between two subsequent strain gages can be written as a function of the difference of measured strains as:

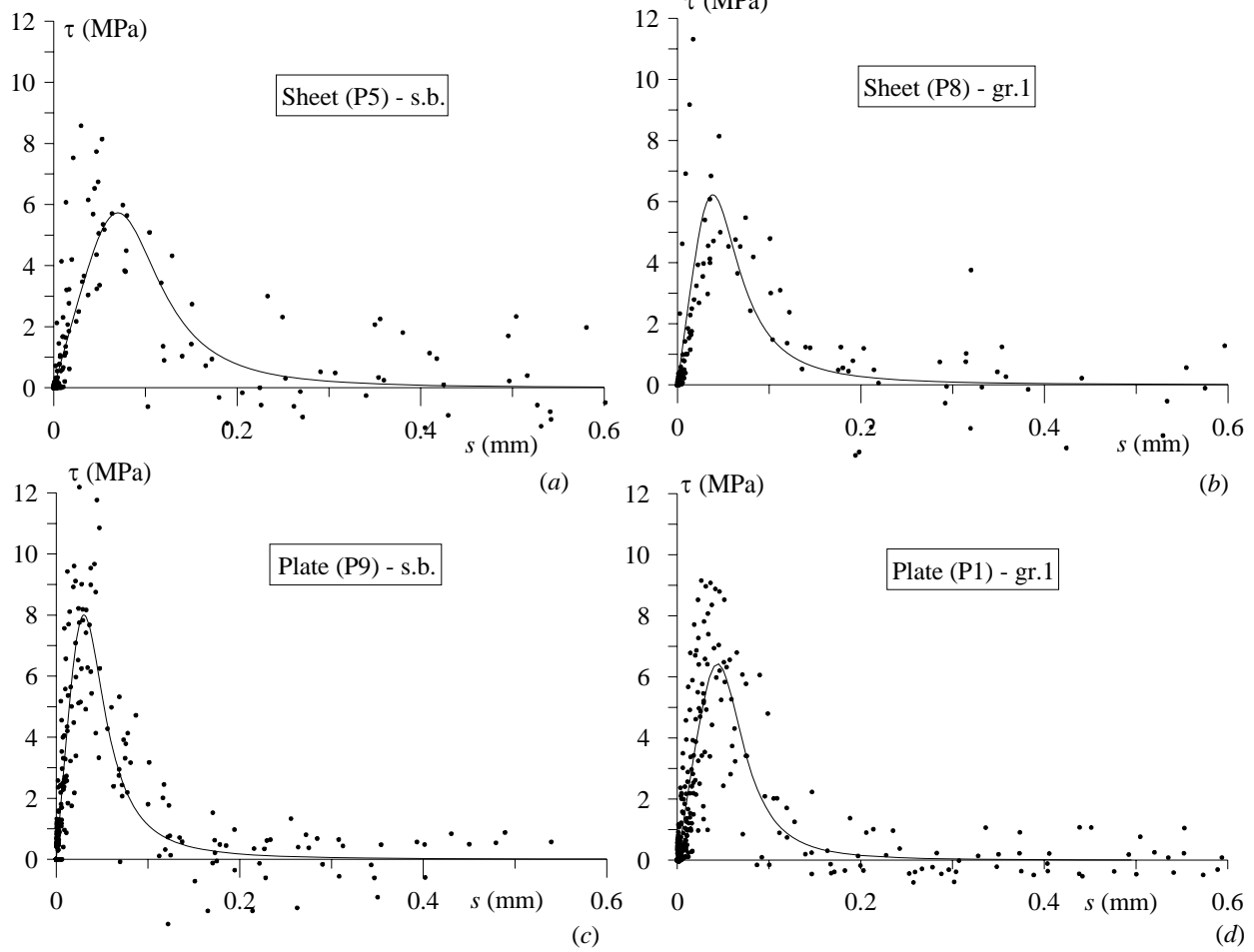


Figure 7. (a, b, c) Shear stress-slip data and interpolation curves by post-processing experimental results for different specimens; (d) comparison of interface laws (s.b.= sand blasting, gr. 1= grinding with stone wheel with marble powder).

$$\bar{\tau}_{i+1/2} = \frac{E_p A_p (\varepsilon_{i+1} - \varepsilon_i)}{b_p (x_{i+1} - x_i)}, \quad (2)$$

with A_p , E_p being cross-section and elastic modulus of the composite. Moreover, assuming perfect bonding (no slip) at the end of bonded plate, integration of the strain profile gives the following expression for the slip at x , with $x_i \leq x \leq x_{i+1}$:

$$s(x) = s(x_i) + \frac{(\varepsilon_{i+1} - \varepsilon_i)}{(x_{i+1} - x_i)} \frac{x^2}{2} + \varepsilon_i x, \quad (3)$$

where $s(0)=0$ is assumed. Average value $\bar{s}_{i+1/2}$ of slip between x_i , x_{i+1} is then computed.

6 CALIBRATION OF A NON LINEAR INTERFACE LAW

According to the procedure described in Savoia et al. (2003), shear stress – slip data are used to calibrate a non linear FRP – concrete interface law. In particular, the interface law recently proposed by the authors (Savoia et al. 2003, Ferracuti et al. 2007b):

$$\tau = \bar{\tau} \frac{s}{\bar{s}} \frac{n}{(n-1) + (s/\bar{s})^n} \quad (4)$$

is adopted, where $\bar{\tau}$ is the peak shear stress, \bar{s} the corresponding slip, and n is a parameter mainly governing the softening branch. Values of $n > 2$ are required in order to obtain positive and finite values of fracture energy.

All shear stress – strain data ($\bar{\tau}_{i+1/2}$, $\bar{s}_{i+1/2}$) related to both experiments conducted for every specimen are grouped together (Fig. 7). Moreover, fracture energy G_f estimated from the mean value of maximum transmissible force (see Equation 1) is used as a constraint. A least square minimization between theoretical and experimental shear stress – strain data is then performed to evaluate the three unknown parameters of interface law in Equation 4, i.e., $\bar{\tau}$, \bar{s} , n . Further details on numerical procedure can be found in Savoia et al. (2003) and Ferracuti et al. (2007b).

In Figures 7a-d, shear stress-slip data are reported, together with the corresponding interface law. It is worth noting that the proposed law is in good agreement with experimental data both for

slips smaller than \bar{s} and in the softening branch where experimental results are more scattered. Values of interface law parameters obtained from calibration procedure are reported in Table 5. Moreover, in Figure 8, three different interface laws are compared.

With reference to FRP sheet bonded to concrete, it can be verified that sand blasting reduces significantly interface stiffness (about one half) and slightly peak shear stress. Nevertheless, softening branch is less brittle, and corresponding fracture energy is 40 percent greater.

Finally, interface laws obtained from delamination tests on FRP sheet and plates, both with concrete surface sand blasted before resin application, are very different, even if their fracture energies are very close. Plate – concrete interface is much stiffer than sheet – concrete counterpart (more than three times greater), with higher value of peak shear stress but brittle softening branch. This is probably due to the significantly higher in-plane stiffness with respect to FRP sheet.

Differences on stiffness of initial branch of interface laws may have some significant consequences in some applications, because the smaller the initial stiffness, the larger the effective bond length required to transmit the full bonding force.

7 CONCLUSIONS

Results from a set of experimental delamination tests on FRP – concrete specimens with different concrete surface preparation before bonding are presented. Bonding of both CFRP plates and sheets have been tested. A particular set-up has been adopted, allowing for a stable delamination process. Applied force, displacements and strains along FRP plate have been measured. The delamination force is used to estimate the fracture energy of interface law.

Non linear interface shear stress – slip laws have

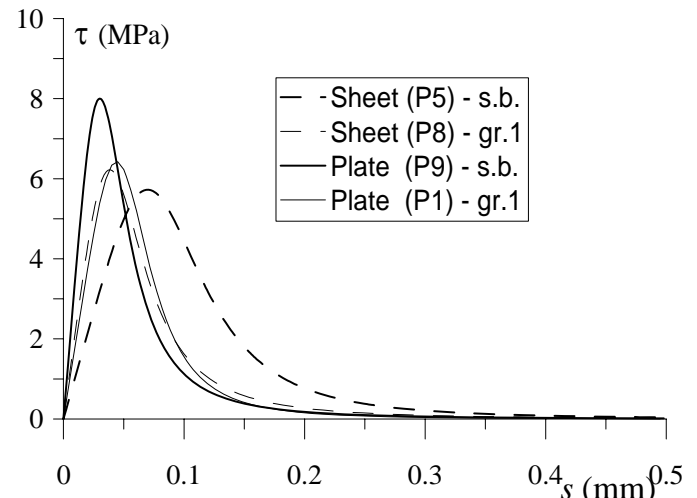


Figure 8. Comparison between interface laws obtained from delamination tests on plate/sheets with different concrete surface preparation (s.b.=sand blasted, gr.1=type 1 grinding).

Table 5. Parameters of interface laws for different concrete surface preparations.

	$\bar{\tau}$ (MPa)	\bar{s} (mm)	n
Sheet (P5) – sand blasted	5.72	0.069	4.2535
Sheet (P8) – grinded 1	6.22	0.038	3.6862
Plate (P9) – sand blasted	8.00	0.030	3.7063
Plate (P1) – grinded 1	6.43	0.044	4.4370

also been calibrated starting from experimental data, adopting the value of fracture energy as a constraint in the minimization procedure between experimental and predicted values.

It is shown that sand blasting of concrete surface before resin application increases delamination force (15-20 percent in the present study), even if it reduces peak shear stress and stiffness of initial branch of interface law.

ACKNOWLEDGEMENTS

The authors would like to thank the Sika Italia S.p.A. for providing CFRP plates and adhesives for the specimens. Financial support of Department of Civil Protection (Reluis 2005 Grant – Task 8: Innovative materials for vulnerability mitigation of existing structures) and C.N.R., PAAS Grant 2001 are gratefully acknowledged.

REFERENCES

- Arrea, M. & Ingraffea, A.R. 1982. Mixed-mode crack propagation in mortar and concrete, Dept. of Structural Engineering, Cornell University, Report n. 81-13.
- Bazant, Z.P. & Pfeiffer, P.A. 1986. Shear fracture tests of concrete. *Materials and Structures*, 19: 111-121.
- Brosens, K. 2001. Anchorage of externally bonded steel plates and CFRP laminates for the strengthening of concrete elements. *Doctoral thesis*, University of Leuven, Belgium.
- Buyukozturk, O., Gunes, O. & Karaca, E. 2004. Progress on understanding debonding problems in reinforced concrete and steel members strengthened using FRP composites - Short survey, *Construction and Building Materials*, 18(1): 9-19.
- CNR Committee 2006. Guide for the Design and Construction of Externally Bonded FRP Systems for Strengthening Existing Structures, *CNR DT 200/2004 Technical Report*.
- Ferracuti, B., Savoia, M. & Mazzotti, C. 2006. A numerical model for FRP-concrete delamination. *Composites Part B: Engineering*, 37(4-5): 356-364.
- Ferracuti, B., Martinelli, E., Nigro, E. & Savoia, M. 2007a. Fracture energy and design rules against FRP-concrete debonding. In T. Triantafillou (ed.), *Proc. of FRPRCS-8 Conference*, Patras, Greece, July 2007.
- Ferracuti, B., Savoia, M. & Mazzotti, C. 2007b. Interface law for FRP-concrete delamination. *Composite Structures*, in press.
- Freddi, F., Salvadori, A. & Savoia, M. 2004. Boundary element analysis of FRP-concrete delamination, In C.A. Brebbia (ed.) *Boundary elements; Proc. int. Symp.*, Southampton, 26: 335-344.
- Galecki, G., Maerz, N., Nanni, A. & Myers, J. 2001. Limitations to the use of waterjets in concrete substrate preparation. In *American waterjet conference; Proc. of WJTA*, Minneapolis, Minnesota, USA, 2001: 1-6 (on CD).
- Lu, X.Z., Teng, J.G., Ye, L.P. & Jiang, J.J. 2005. Bond-slip model for FRP sheets/plates bonded to concrete, *Engineering Structures*, 27: 920-937.
- Matana, M., Galecki, G., Maerz, N. & Nanni, A. 2005. Concrete substrate preparation and characterization prior to adhesion of externally bonded reinforcement. In J.F. Chen & J.G. Teng (eds.), *International symposium on bond behaviour of FRP in structures; Proc. of BBFS*, Hong Kong, December 2005: 1-7 (on CD).
- Mazzotti, C., Ferracuti, B. & Savoia, M. 2004. An experimental study on FRP – concrete delamination. In Li et al. (eds.), *Proc. FraM-CoS-5*, Vail (CO), 2: 795-802.
- Savoia, M., Ferracuti, B. & Mazzotti, C. 2003. Non linear bond-slip law for FRP-concrete interface, In K.H. Tan (ed.), *Proc. of FRPRCS-6 Conference*, Singapore: 1-10.
- Toutanji, H., Ortiz, G. 2001. The effect of surface preparation on the bond interface between FRP sheets and concrete members. *Composite Structures*, 53: 457-462.
- Van Mier, J.G.M. 1997. *Fracture processes of concrete*, Boca Raton: CRC Press.
- Yao, J., Teng, J.G., Chen, J.F. 2005. Experimental study on FRP-to-concrete bonded joints. *Composites Part B: Engineering*, 36(2): 99-113.